World Journal of Advanced Engineering Technology and Sciences
eISSN: 2582-8266
Cross Ref DOI: 10.30574/wjaets
Journal homepage: https://wjaets.com/

(RESEARCH ARTICLE)

Check for updates

Parameter optimization of high energy ball milling process for TiO_2 powder using the Taguchi method

Maya Radune [1,*], Svetlana Lugovskoy [2], Yaniv Knop [1] and Barbara Kazanski [3]

[1] *Department of Civil Engineering, Ariel University, Ariel, Kiryat Hamada, 40700, Israel.*
[2] *Department of Chemical Engineering, Ariel University, Ariel, Kiryat Hamada, 40700, Israel.*
[3] *Department of Materials Engineering, Azrieli College of Engineering, Jerusalem, 91035000, Israel.*

World Journal of Advanced Engineering Technology and Sciences, 2024, 12(01), 390–403

Publication history: Received on 13 April 2024; revised on 05 June 2024; accepted on 08 June 2024

Article DOI: https://doi.org/10.30574/wjaets.2024.12.1.0218

Abstract

The Taguchi method's robust design was applied to investigate the effect of main high-energy ball milling (HEBM) parameters – milling time (MT), ball-to-powder weight ratio (BPWR), and milling speed (MS) – on the TiO_2 crystallite size (CS). The experiment used the $L_{16}(4^3)$ orthogonal array (OA). The as-received and milled powders were characterized by X-ray diffraction (XRD) and scanning electron microscopy (SEM). The CS of TiO_2 varied between 3.48 and 73.70 nm depending on the HEBM conditions. The optimum milling parameter combination was determined by using the analysis of signal-to-noise (S/N) ratios. Based on the S/N ratio ana-lysis, optimal HEBM conditions were found to be MT 100h, MS 400rpm, BPWR 50:1. The analysis of variance (ANOVA) was used for indicating the significance of each milling parameter and their effect on CS. Statistical analysis by S/N and ANOVA established that the MT is the most influential parameter, followed by MS and BPWR. The results of the parameter optimization experiment were validated by a confirmation test at a 90% confidence level. The confirmation test showed that there is a good agreement between the experimental and statistical data.

Keywords: High-energy ball milling; Titanium Dioxide powder; Taguchi technique; Orthogonal array; Signal-to-noise ratio ANOVA; Confidence interval; Nanoparticle

1. Introduction

In the search for modern and innovative construction materials and technologies, their durability, aesthetics, and environmental impact are very important factors [1, 2]. Concrete is the most commonly used material in civil engineering. The choice is justified not only by the resulting durability and aesthetics of buildings; its properties, which actively support environmental protection, have also become one of the most important arguments for the application of this material. The incorporation of nanosized particles of titanium dioxide (TiO_2) into cementitious materials further enhances the ecological value of concrete [3]. The use of cement with TiO_2 additives in the composition of the concrete mix reduces harmful compounds present in the air surrounding the concrete buildings, as well as enabling removal of impurities which occur on the concrete surfaces over time. It is worth emphasizing that in addition to reduced air pollution by active surfaces of concrete made with cement including TiO_2, concrete also has self-cleaning properties. According to research [4], concrete triggers the degradation of almost all organic substances liable to come in contact with it.

Some factors that affect physical and chemical TiO_2 properties are its crystalline structures, specific surface area, crystallite size (CS), and particle size [5, 6]. The factors affecting the properties of TiO_2 can be modified by preparation

* Corresponding author: Maya Radune

methods such as pulsed laser ablation [7], sol-gel [8], solvothermal synthesis [9], precipitation [10], and plasma spraying [11, 12].

The mechanical ball milling technique is well known as a simple and low-cost method for the production of submicron or nanostructured materials with the possibility of obtaining large quantities [13-15]. Ball milling is used for grinding all kinds of materials [16, 17]. High-energy ball milling (HEBM) is a process involving a number of independent and interdependent variables. Many parameters have been tested to optimize the ball milling process, such as milling speed (MS), milling time (MT), ball sizes, ball-to-powder weight ratio (BPWR), and the milling medium [18-25].

However, there is currently no conclusive method to determine the best parameters applied to the ball milling process to transform macro-size materials to nano-scale particles. Hence, identifying the parameters contributing to the desired particle sizes and crystal structures of the milled powder is important.

The traditional experimental design methods are too complex, time-consuming, and complicated to apply. Many more experiments must be carried out as the number of process parameters increases. Statistical experimental designs provide an easier and more efficient approach to optimize functional variables. The Taguchi method is one of the robust designs widely used in the field of engineering to determine the optimum process parameters [26-29]. Compared to the factorial method, which requires testing all possible combinations of available parameters, the Taguchi method provides a more simplified way to set up the combination of experimental parameters [30, 31].

This study aimed to determine the effect of HEBM parameters (MS, MT, and BPWR) on the CS of TiO_2 powder by applying the Taguchi method. These parameters were optimized according to the calculated S/N ratio of parameters. Moreover, ANOVA was employed for evaluating the statistical significance and relative contributions of these HEBM parameters. Each milled powder was characterized using XRD and SEM.

2. Materials and Methods

TiO_2 powder (99.9% purity, Sigma Aldrich) was used as the starting material. The morphology of this powder is shown in Figure 5.1. The raw TiO_2 particles were micron size and irregular in shape. The TiO_2 powder was milled by HEBM in a planetary ball mill (Retsch PM 100, Germany) using a container (250 ml volume) and balls (10 mm diameter) made from chromium-hardened steel. The milling was performed at room temperature and followed different milling parameters (see Table 4.1).

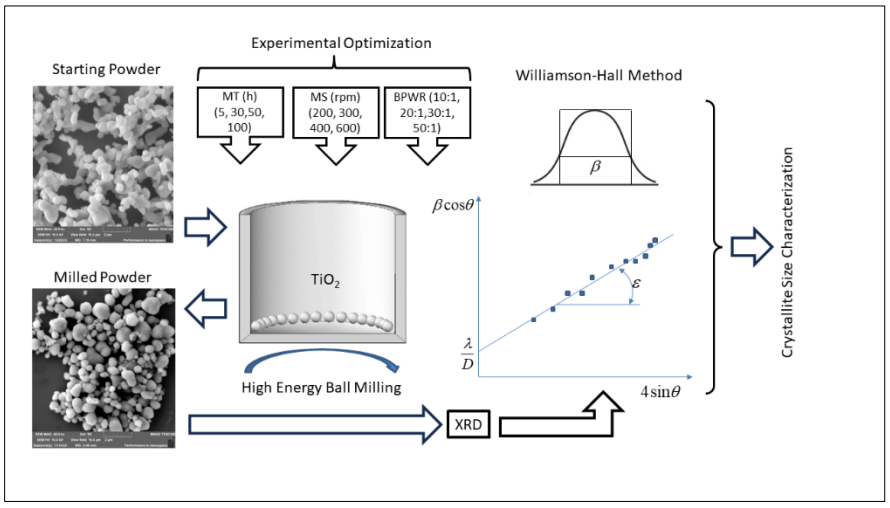

Figure 1 Diagram depicting the preparation of TiO_2 nanoparticle powder by design optimization

-The structural evolutions and phase analysis of the milled powders were characterized by XRD testing (Panalytical X'Pert Pro X-ray diffractometer) with CuK_α radiation (λ=0.154 nm), operating at 40 kV and 40 mA. Data collection was performed by step scanning of the specimen over the 2θ : $20 - 70^\circ$ angular range, in steps of 0.05° with 3 sec per step. The XRD line profile parameters were fitted with Rietveld refinement, using the PANalytical X'Pert HighScore Plus v3.0e software. The CS of the milled powders were determined by a broadening of XRD peaks using the Williamson-Hall (WH) method [32].

The morphology of the initial and milled powders was examined using STEM (MAIA3 TESCAN). The Taguchi experimental design was used to find the optimal level of the main milling parameters and their effect on the CS of TiO_2 powder. Fig. 1 depicts the process optimization through the HEBM process.

2.1. Taguchi Method

The Taguchi method which was used in this study is briefly described below.

The signal factor (S) and noise factor (N) accompanied by the relevant level are selected. Signal factors are input parameters which can be changed in order to achieve optimal conditions in laboratory experiments, by identifying selected levels for the experiment matrix. Noise factors refer to all those that cause changes in the conditions; they were assumed to be constant during our experiment.

The loss functions (L) are calculated to determine modifications of the experimental results to approach the optimal values. Depending on the circumstances, these functions are calculated using the following equations:

'Smaller is better':

$$SB = \frac{1}{n}\sum_{i=1}^{n} y_i^2 \quad \text{.....(1)}$$

'Larger is better':

$$LB = \frac{1}{n}\sum_{i=1}^{n} \frac{1}{y_i^2} \quad \text{.....(2)}$$

'Nominal is best':

$$SB = \frac{1}{n}\sum_{i=1}^{n} \left(y_i - y_0\right)^2 \text{,.....(3)}$$

where n is the number of experiments in the orthogonal array (OA), y_i is the i^{th} measured value, and y_0 is the optimal nominal size.

The total value of S/N can be calculated for each parameter based on the following equation:

$$S/N = -10\log L \text{,.....(4)}$$

The S/N ratio is calculated for each level of the parameters. In the Taguchi method, parameters with the highest S/N ratio (regardless of the type of loss functions) are introduced as optimal levels.

The significance of each parameter is determined using ANOVA.

2.2. Experimental Design

The Taguchi parameter design approach was applied for optimization of the process variables in the HEBM of TiO_2. Many parameters are used in the ball milling process. However, the parameters tested most often for optimization are the MS, MT, and BPWR [33]. This indicates that these three parameters are known to play an important role in determining the effectiveness of the milling. Yet previous work has shown no conclusive evidence for their optimal values [34]. Hussain reported that BPWR is recognized as one of the most influential parameters, along with ball mill working capacity and rotation speed [35]. Zhang et al. believed that the volume of milling medium is the most influential parameter, followed by the rotation speed [35]. Moreover, the BPWR used by previous works clearly varied; although most ratios were in the range from 10:1 to 20:1 [36], some studies used much higher ratios, up to 100:1 [37]. Higher BPWR helps increase the particle size reduction rate. However, when the ratio is too high, there is a possibility of contamination resulting from the collision of grinding balls with the inner wall of the milling vial. There is no conclusive decision on the best BPWR. Some researchers reported the best result at 20:1 or 15:1, while others recommended a lower BPWR of 10:1, or a higher BPWR of at least 50:1 [38, 18]. Therefore, the BPWRs used in our research were 10:1, 20:1, 30:1, and 50:1. Hajalilou et al. [39] claimed that the duration of mechanical alloying is one of the fundamental parameters usually exploited to achieve a steady state between the breaking and rewelding (cold-working) of powder

particles. The refinement of mean particle size during a milling process can be stated as follows, with this relationship applying a simple model for the refinement of nanocrystalline particle size [34]:

$$D = Kt^{-\frac{2}{3}} \text{.....(5)}$$

where t is the milling time, D is the particle size, and K is the constant.

However, as mentioned by Suryanarayana [34] earlier, since a number of process variables could influence the achieved particle size, more systematic experiments are needed before solid explanations can be made. For our purposes, four milling times were chosen: 5, 30, 50, and 100h. Another parameter that has high influence on milling effectiveness is the MS. Almost all researchers used high MS of more than 100 rpm. In fact, a milling speed as high as 2000 rpm was used by Bilgili et al. [40]. Higher milling speed provides higher impact energy exerted by the grinding balls on the materials, resulting in more effective milling [19]. In the current research, all four speeds of the ball mill were used: 200, 300, 400, and 600 rpm. Table 1 shows the parameters selected and the levels for each parameter.

Table 1 Process parameters and their levels

Levels / Parameter	1	2	3	4
MT[h]	5	30	50	100
MS, [rpm]	200	300	400	600
BPWR	10:1	20:1	30:1	50:1

The Taguchi method uses an orthogonal array (OA) to design the experiments. From the parameter design-OA selector shown in Table 2, the selected array was $L_{16}(4^3)$.

Table 2 Parameter design orthogonal array selector [41]

Number of Level	Number of parameters (P)							
	2	3	4	5	6	7	8	9
2	4	4	8	8	8	8	12	12
3	9	9∗	9	18	18	18	18	27
4	’16	’16	’16	’16	’32	’32	’32	’32
5	25	25	25	25	25	50	50	50

The $L_{16}(4^3)$ array parameter configuration is shown in Table 3, while the experimental parameters and levels for each experiment in $L_{16}(4^3)$ array are shown in Table 4.

Table 3 $L_{16}(4^3)$ OA

Experiment Number	Parameter 1	Parameter 2	Parameter 3
1	1	1	1
2	1	2	2
3	1	3	3
4	1	4	4
5	2	1	2
6	2	2	1
7	2	3	4
8	2	4	3

9	3	1	3
10	3	2	4
11	3	3	1
12	3	4	2
13	4	1	4
14	4	2	3
15	4	3	2
16	4	4	1

Table 4 The experimental layout of the $L_{16}(4^3)$ OA

Experiment Number	MT, [h]	MS, [rpm]	BPWR
1	5	200	10:1
2	5	300	20:1
3	5	400	30:1
4	5	600	50:1
5	30	200	20:1
6	30	300	10:1
7	30	400	50:1
8	30	600	30:1
9	50	200	30:1
10	50	300	50:1
11	50	400	10:1
12	50	600	20:1
13	100	200	50:1
14	100	300	30:1
15	100	400	20:1
16	100	600	10:1

The Taguchi methodology was applied for the three factors selected, without considering the interaction effects between them. If the interaction effect is considered in the experiment, a higher OA must be selected. The small size of the experiments, and the fact that they seem to provide satisfactory results, are two reasons that orthogonal arrays are preferred for experimental designs. Sixteen trial runs with certain factor level combinations determined from the array were carried out randomly and repeatedly. Qualitek-4 software was used to assist in selecting the runs in the experimental design in a random order. The experiments were replicated three times for statistical purposes. Thus, $16 \cdot 3 = 48$ were required. This was far less than the $3 \cdot (4^3) = 192$ experiments that would be needed according to a full factorial design.

The verification of results was achieved by running experiments as confirmation tests at the predicted optimal conditions.

All calculations were analyzed using Qualitek-4 software.

3. Results and Discussion

The typical morphologies ultrasonically dispersed in the starting and milled powders are presented below.

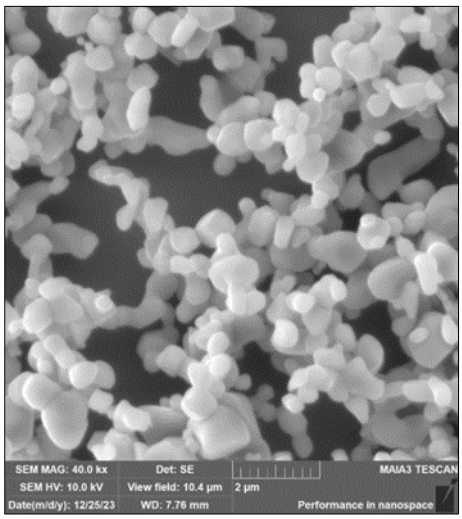

Figure 2 SEM image of starting TiO_2 powder

Unmilled (as-received) TiO_2 powder (Fig. 2 above) consisted of particles with various shapes (spherical, elongated, and irregular). The SEM images of the typical milled TiO_2 powders are shown in Fig. 3 below. Particle sizes significantly decreased after HEBM of 5 h, MS 600 rpm and BPWR 50:1 (Fig. 3(4)), yielding fine particles that formed agglomerates. To explain this phenomenon, one can consider the fact that the ball milling process leads to the refinement of particle size by breaking and rewelding the powder particles; and after a certain (critical) energy is transferred to the particles, they stick together and become agglomerated. Particle size after prolonged treatment and greater MS and BPWR remained almost constant, whereas the level of agglomeration increased considerably (Fig. 3 (7-13)).

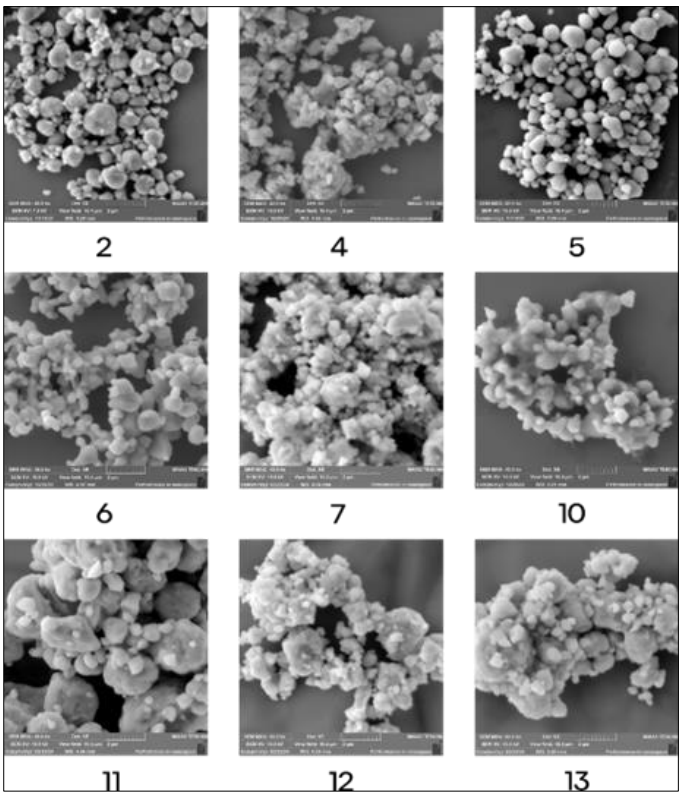

Figure 3 SEM images of milled TiO_2 powder. The numbers indicate the experiment

The XRD patterns of the milled powders, obtained by applying the L_{16} OA in the Taguchi design, are shown in Figure 4. The Bragg diffraction peaks were shown to be broadened and reduced in intensity, which can be related to the crystallite size reduction and the internal strain in the milling powder. WH analysis showed that the strain of the milled powders was above zero (0-0.37%); therefore, the broadened peaks indicated crystallite size only. Originally the milled powder was identified as rutile. Following the HEBM, part of the rutile's phase remained as rutile and part of it was transformed into a mixture of rutile, anatase and Ti_3O_5 phases, depending on the intensity of the milling conditions. Additionally, the milled powder contained a significant fraction of Fe and (Ti, Fe) O which originated from the steel grinding medium. The position of these peaks did not change with milling.

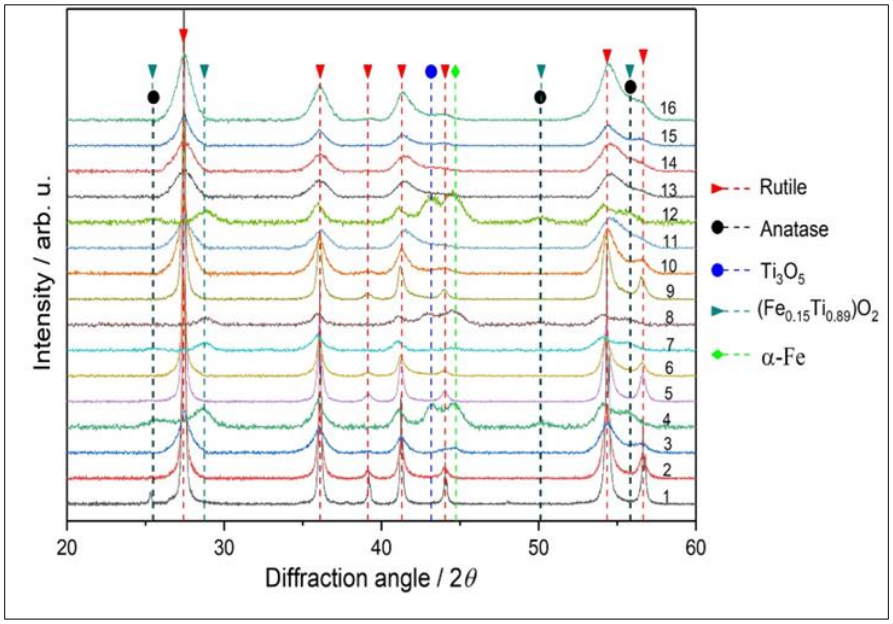

Figure 4 XRD patterns of milled TiO_2 powder. The numbers from 1 to 16 indicate the experiment number

The average crystallite sizes of TiO_2, obtained in three repeated experiments for each of the sixteen trial conditions, are presented in Table 5. They are in the range of 3.48-73.70 nm. Each sample had its own conditions (different BPWR, MS, and MT) which caused changes in the XRD peaks. Note that each of the selected parameters affected the changes in peaks independently, which was the number analyzed in the Taguchi procedure.

Table 5 The TiO_2 average crystallite sizes and S/N ratios (replicated 3 times)

Experiment Number	Average crystallite size, nm	S/N ratio, DB
1	73.7	-37.35
2	49.81	-33.95
3	8.63	-18.72
4	6.78	-16,63
5	29.68	-29.45
6	16.10	-24.14
7	6.58	-16.37
8	9.46	-19.52
9	70.70	-36.99
10	6.70	-16.52
11	3.48	-10.83

12	6.17	-15.81
13	3.87	-11.76
14	3.88	-11.78
15	8.02	-18.08
16	6.3	-15.99

3.1. Statistical optimization

The value of signal-to-noise ratio (S/N) was used to determine the optimal and most influential parameters relating to the crystallite size of TiO_2 HEBM powder. In this experiment, the S/N was used to identify the control factors that reduce the variability of the results by minimizing the effects of uncontrollable factors. The S/N ratio formula (Eq. 4) for the static design was divided into three categories: 'nominal is best', 'larger is better', and 'smaller is better' [42]. Because lower crystallite size was desirable, a 'smaller is better' formula (Eq. 6) was chosen for the analysis of the experimental results:

$$S/N = -10\log\left[\frac{1}{n}\sum_{i=1}^{n} y_i^2\right] \text{.....(6)}$$

The computed S/N ratios are presented in Table 5. As shown in Eq. 6, from the qualitative objective of 'smaller is better', which is to minimize the CS, a greater S/N ratio corresponds to a smaller variance of the output characteristic around the desired value. The differences between obtained values were strongly dependent on the milling conditions. Since the experimental design is orthogonal, it was possible to separate the effect of each parameter at different levels [42]. To do this, the mean S/N ratio was determined for each parameter and level. The mean S/N ratio is the average of the S/N ratio for each parameter at different levels [43]. For example, the effect of MS at level 1 (MS_1 ; experiments 1, 5, 9, and 13) was calculated as follows: $MS_1 = \frac{1}{4}\left(\frac{S}{N_1} + \frac{S}{N_5} + \frac{S}{N_9} + \frac{S}{N_{13}}\right)$. The results are tabulated in Table 6, also known as the S/N response table.

Table 6 Response table for TiO_2 crystallite size

Level	**MT**	**MS**	**BPWR**
1	-26.66	-28.89	-22.08
2	-22.37	-21.60	-24.32
3	-20.04	−16.00*	-21.75
4	−14.40*	-16.98	−15.32*
Delta Δ	12.26	12.89	9.01
Rank	2	1	3

* Optimum parameter level.

The difference between maximum and minimum S/N ratios (Δ) determines the main effect of the parameter. With greater (Δ) values, the effect of the parameter on the process will correspond to a smaller variance of the output, thus generating better performance in the experiment [44]. From the point of the 'smaller is better' qualitative characteristic, the MS had the largest effect (Δ = 12.89) on the TiO_2 CS, while BPWR had the smallest effect (Δ = 9.01).

A parameter level corresponding to the maximum average S/N ratio is the optimal level for that parameter [45]. Based on the S/N ratio analysis, the optimal conditions for smaller TiO_2 CS were: MS_3 (400 rpm), MT_4 (100 h) and $BPWR_4$ (50:1) (Fig. 5). Table 7 summarizes the optimum parameters calculated.

Table 7 Optimum parameters

Parameter	Level	Description
MS	3	400rpm
MT	4	100h
BPWR	4	50:1

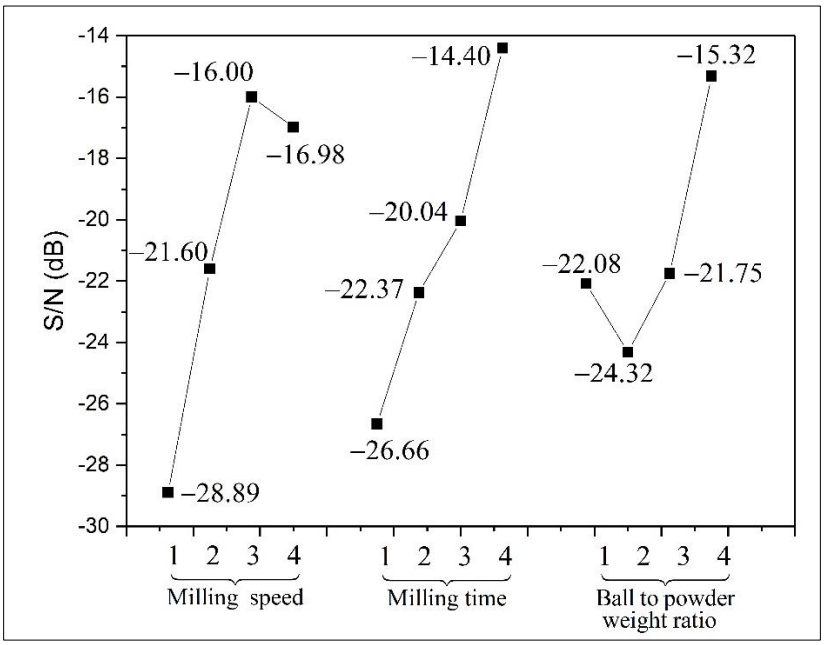

Figure 5 Main effect of process parameters on S/N

3.2. Statistical analysis of variance (ANOVA)

The Taguchi method cannot judge and determine the effect of individual parameters on the entire process, but the percentage contribution of individual parameters can be determined using analysis of variance (ANOVA) based on the F-statistics test (Eqs. 7-12) [46]. The primary purpose of applying ANOVA is to investigate which design parameters significantly affected the qualitative characteristic. Thus, it can be decided which independent factor dominated another, and the percentage contribution of that particular independent variable. The analysis measures the sum of the squared deviations from the total mean S/N, to determine which parameters significantly affected the crystallite size of the TiO_2 milling powder. The F-ratio is the ratio of the mean square error to the residual error and is traditionally applied to determine the significance of a factor [47].

$$SS_{Total} = \sum X^2 - \frac{\left(\sum X\right)^2}{N} \quad \text{.....(7)}$$

$$SS_{Between} = \frac{\left(\sum X_1\right)^2}{n_1} + \frac{\left(\sum X_2\right)^2}{n_2} + \ldots + \frac{\left(\sum X_n\right)^2}{n_n} \quad \text{.....(8)}$$

$$DF = N - 1 \quad \text{.....(9)}$$

$$SS_{Within} = SS_{Total} - SS_{Between} \quad \text{.....(10)}$$

$$F - Calculated = \frac{MSG}{MSE} \text{ .....(11)}$$

$$\%Contribution = \frac{MS}{MS_{Total}} \text{ .....(12)}$$

where 'SS' is sum of squares, 'DF' is degree of freedom, 'N' is total observations, and 'n_i' is size of the population.

Qualitek-4 software in the ANOVA module was employed to investigate the effect of process parameters. ANOVA results are presented as standard ANOVA tables, and the results for the CS and S/N are given in Tables 8 and 9 respectively.

Table 8 ANOVA table for TiO_2 crystallite size

Factor	DOF (f)	Sum of Squares(S)	Variance (V)	F-Ratio (F)	Pure Sum (S)	Contribution, P(%)
MS	3	1795.49	598.50	1.78	789.37	9.25
MT	3	3762.82	1254.27	3.74	2756.71	32.31
BPWR	3	962.30	320.77	0.96	0	0
Other error	6	2012.23	335.37	-	-	58.44
Total	15	8532.85	-	-	-	100

Table 9 ANOVA table for S/N ratio

Factor	DOF (f)	Sum of Squares(S)	Variance (V)	F-Ratio (F)	Pure Sum (S)	Contribution, P(%)
MS	3	313.26	104.42	2.35	179.98	15.33
MT	3	414.37	138.12	3.11	281.09	23.94
BPWR	3	179.88	59.96	1.35	46.60	3.97
Other error	6	266.56	44.43	-	-	56.76
Total	15	1174.08	-	-	-	100

The F-value for this condition, with 90% confidence, is 3.1 [48]. The results showed that only the MT had significant effect on the CS. The F-value of this factor was greater than the extracted F-value from the table, at a 90% confidence level. Hence, the variance of this factor was significant compared with the variance of error. The F-values for MS and BPWR were less than 3.1, which were not statistically significant factors (at least not in the range under study). Since the model's F-value was less than the extracted F-value from the table at a 90% confidence level, this model was not meaningful. In order to obtain a meaningful model, a pooled ANOVA was performed. Taguchi's rule for pooling requires starting with the smallest main effect and successive inclusion of larger effects. The values of the ANOVA for the CS and S/N after pooling of the MS and BPWR are shown in Tables 10 and 11.

Table 10 Pooled ANOVA table for TiO_2 crystallite size

Factor	DOF (f)	Sum of Squares(S)	Variance (V)	F-Ratio (F)	Pure Sum (S)	Contribution, P(%)
MT	3	3762.82	1254.27	3.74	2756.71	32.31
Other error	12	4770.02	397.50	-	-	67.69
Total	15	8532.85	-	-	-	100

Table 11 Pooled ANOVA table for S/N ratio

Factor	DOF (f)	Sum of Squares(S)	Variance (V)	F-Ratio (F)	Pure Sum (S)	Contribution, P(%)
MT	3	414.37	138.12	3.11	281.09	23.94
Other error	12	759.76	63.31	-	-	76.06
Total	15	1174.13	-	-	-	100

The ANOVA results closely matched the Taguchi ones. The F-value for pooled condition at a 90% confidence level is 2.7 [48]. The model F-values 3.74 and 3.11 for CS and S/N, respectively, implied that the model was significant.

3.3. Prediction of CS under optimal conditions

The crystallite size was predicted at the optimal levels of milling parameters: MS_3, MT_4 and $BPWR_4$ (note that MS and BPWR are pooled factors) (Eq.13):

$$u_0 = y_m + \sum_{i=1}^{n}\left(y_j - y_m\right) \text{.....(13)}$$

where y_m is the total mean of the CS y, n is the number of main milling parameters which significantly affect performance, and y_j is the mean measured value for j^{th} milling parameters corresponding to the optimal parameter level.

Under these conditions, the predicted CS was computed as 6.68 nm.

Since Eq.13 is a point estimation, which is calculated by using experimental data to determine whether or not the results of the confirmation experiments are meaningful, the confidence interval (CI) must be evaluated.

The CI was employed here to verify the qualitative characteristics of the confirmation experiments. The CI for the predicted optimal values was calculated as follows (Eq. 14):

$$C.I. = \sqrt{\frac{F_\alpha\left(1, f_e\right)V_e}{n_{eff}}} \text{.....(14)}$$

where $F_\alpha(1, fe)$ is the F-ratio at a 90% confidence level, f_e is the degree of freedom for error, V_e is variance of the error term (from ANOVA Table 10), and n_{eff} is the number of effective measured results. The CI at a 90% confidence level is calculated to be ±16.38. Thus, the optimal TiO_2 crystallite size was estimated with 90% confidence as (6.68 ± 16.38) nm.

3.4. Confirmation Test

With the Taguchi optimization methodology, a confirmation test is required to validate the optimized condition, including the optimal process parameters, in order to show how closely the respective prediction corresponded with the real experiment. The confirmation test is highly recommended by Taguchi to verify the accuracy of the optimal process parameters that have been selected. Three confirmation runs were conducted under the predicted optimal conditions (MS_3, MT_4, and $BPWR_4$). The average TiO_2 crystallite size was found to be 3.25 nm. This result was within a 90% CI for the predicted optimal TiO_2 crystallite size value. Therefore, the confirmation tests indicated successful optimization.

4. Conclusions

The Taguchi method was applied to investigate the effect of HEBM parameters on the CS of TiO_2 powder. The HEBM process was analyzed with the Taguchi L_{16} OA. Results obtained from the Taguchi method were analyzed using S/N ratios for identification of optimal parameters. The optimal results were obtained as selected as MT_4 (100h), MS_3 (400 rpm), and $BPWR_4$ (50:1). It was concluded that MT is the most influential parameter, followed by MS and BPWR. It was

revealed that MS and BPWR were not statistically significant factors, at least in the range under study. Based on the ANOVA table, the contribution percentages of the MT, MS, and BPWR were 32.31%, 9.25%, and 0%, respectively, at a 90% confidence level. In addition, the confirmation tests using the predicted optimal parameters demonstrated that the average TiO_2 CS was within the expected range of the values within confidence limits, which identified the results as trustworthy.

Compliance with ethical standards

Acknowledgments

The authors thank Dr. A. Kossenko, Dr. O. Krichevski and Dr. T. Brieder for assistance with XRD and SEM.

Disclosure of conflict of interest

The authors declare that they have no conflicting interests.

References

[1] Langier B (2012). Fly ash from processes of coal co-combustion with alternative fuels in concrete technology. In Proceedings of the 4th International Conference on Contemporary Problems in Architecture and Construction., pages 310–315, Czestochowa University of Technology. Sustainable Building Industry of the Future.

[2] Pietrzak A (2014). Environment-friendly technologies in the construction industry as an example of "green concrete" - the use of sewage sludge for the production of concrete. Construction of optimized energy potential, Czestochowa University of Technology, 1(13), 86–93.

[3] Pietrzak A, Adamus J, and Langier B (2016). Application of titanium dioxide in cement and concrete technology. Key Engineering Materials, 687, 243–249.

[4] Guerrini G (2010). Photocatalytic cementitious materials – situation, challenges and perspectives. World Cement, pages 1–4.

[5] Retamoso C, Escalona N, Gonz´alez M, Barrientos L, Allende-Gonz´alez P, Stancovich S, Serpell R, Fierro J, and Lopez M (2019). Effect of particle size on the photocatalytic activity of modified rutile sand (TiO_2) for the discoloration of methylene blue in water. J. Photochem. Photobiol. Chem., 378, 136–141.

[6] Suwannaruang T, Kamonsuangkasem K, Kidkhunthod P, Chirawatkul P, Saiyasombat C, Chanlek N, and Wantala K (2018). Influence of nitrogen content levels on structural properties and photocatalytic activities of nanorice-like n-doped TiO_2 with various calcination temperatures. Mater. Res. Bull., 105, 265–276.

[7] Zhou R, Lin S, Zong H, Huang T, Li F, Pan J, and Cui J (2017). Continuous synthesis of Ag/TiO_2 nanoparticles with enhanced photocatalytic activity by pulsed laser ablation. J. Nanomater., 2017, https://doi.org/10.1155/2017/4604159.

[8] Giampiccolo A, Tobaldi D, Leonardi S, Murdoch B, Seabra M, Ansell M, Neri G, and Ball R (2019). Sol gel $graphene/TiO_2$ nanoparticles for the photocatalytic-assisted sensing and abatement of NO_2. Appl. Catal. B Environ., 243, 183–194.

[9] Wang F, Pan K, Wei S, Ren Y, Zhu H, Wu H, and Zhang Q (2021). Solvothermal preparation and characterization of ordered-mesoporous ZrO_2/TiO_2 composites for photocatalytic degradation of organic dyes. Ceram. Int., 47, 7632–7641.

[10] Buraso W, Lachom V, Siriya P, and Laokul P (2018). Synthesis of TiO_2 nanoparticles via a simple precipitation method and photocatalytic performance. Mater. Res. Express, 5(11), DOI 10.1088/2053–1591/aadbf0.

[11] Takahashi Y, Shibata Y, Maeda M, Miyano M, Murai K, and Ohmori A (2014). Plasmaspraying synthesis of high-performance photocatalytic TiO_2 coatings. IOP Conf.Ser. Mater. Sci. Eng., 61, DOI 10.1088/1757–899X/61/1/012039.

[12] Zhai M, Liu Y, Huang J, Hou W, Wu S, Zhang B, and Li H (2020). Fabrication of TiO_2-$SrCO_3$ composite coatings by suspension plasma spraying: microstructure and enhanced visible light photocatalytic performances. J. Therm. Spray Technol., 29, 1172–1182.

[13] Koch C (1997). Synthesis of nanostructured materials by mechanical milling: problems and opportunities. Nanostruct. Mater., 9, 13–22.

[14] Muñoz J, Cervantes J, Esparza R, and Rosas G (2007). Iron nanoparticles produced by high-energy ball milling. J. Nanopart. Res., 9, 945–950.

[15] Mahamat A, Rani A, and Husain P (2012). Behavior of $Cu - W\ C - T\ i$ metal composite after using planetary ball milling. International Journal of Engineering and Applied Sciences, 10(8), 278–282.

[16] Wang Y and Forssberg E (2006). Production of carbonate and silica nano-particles in stirred bead milling. International Journal of Mineral Processing, 81(1), 1–14.

[17] Hubert G, Petracovschi E, Zhang X, and Calvez L (2013). Synthesis of germanium-gallium-tellurium ($Ge{-}Ga{-}T\ e$) ceramics by ball-milling and sintering. Journal of the American Ceramic Society, 96(5), 1444–1449.

[18] Radune M, Lugovskoy S, Knop Y, and Yankelevitch A (2022). Use of Taguchi method for high energy ball milling of $CaCO_3$. Mater Eng, 17(1), https://doi.org/10.1186/s40712–021–00140–8.

[19] Radune M, Radune A, Lugovskoy S, Zinigrad M, Fuks D, and Frage N (2014). Mathematical modeling of high energy ball milling (HEBM) process. Defect and Diffusion Forum, 353, 126–130.

[20] Radune M, Zinigrad M, and Frage N (2015). Optimization of high energy ball milling parameters for synthesis of $T\ i_xAl_{1-x}N$ powder. Journal of Nano Research, 38, 107–113.

[21] Davis R and Koch C (1987). Mechanical alloying of brittle components: silicon and germanium. Scripta Metall, 21, 305–310.

[22] Watanabe H (1999). Critical rotation speed for ball-milling. Powder Technol., 104, 95–99.

[23] Enqvist E, Ramanenka D, Marques P, Gracio J, and Emami N (2016). The effect of ball milling time and rotational speed on ultra high molecular weight polyethylene reinforced with multiwalled carbon nanotubes. Polym.Compos., 37, 1128–1136.

[24] Kutuk S (2016). Influence of milling parameters on particle size of ulexite material. Powder Technol., 301, 421–428.

[25] Rizal S, Abdullah C, Olaiya N, Sri Aprilia N, Zein I, Surya I, and Abdul Khalil H (2020). Preparation of palm oil ash nanoparticles: Taguchi optimization method by particle size distribution and morphological studies. Appl. Sci., 10, 985–1000 doi:10.3390/app10030985.

[26] Gopalsamy B, Mondal B, and Ghosh S (2009). Taguchi method and ANOVA: an approach for process parameters optimization of hard machining while machining hardened steel. Journal of Scientific and Industrial Research, 68, 689–695.

[27] Pouretedal H, Fallahgar M, Sotoudeh Pourhasan F, and Nasiri M (2017). Taguchi optimization of photodegradation of yellow water of trinitrotoluene production catalyzed by nanoparticles TiO_2/N under visible light. Iran. J. Catal., 7, 317–326.

[28] Pundir R, Chary G, and Dastidar M (2018). Application of Taguchi method for optimizing the process parameters for the removal of tungsten and nickel by growing aspergillus sp. Water Res. Ind., 20, 83–92.

[29] Francis D, Aiswarya T, and Gokhale T (2022). Optimization and mathematical modeling using Taguchi and regression analysis method for particle size and pdi of WO_3 nanoparticles synthesized by stenotrophomonas maltophilia. Heliyon, 8, e10640.

[30] Ngo M, Hoang V, and Hoang S (2009). Taguchi-fuzzy multi-response optimization in fly cutting process and applying in the actual hobbing process. International Journal of Mechanical and Materials Engineering, pages doi:org/10.1186/s40712–018–0092–z.

[31] Rameswara Y (2023). Optimization of surface roughness and material removal rate in turning using gray based Taguchi approach. World Journal of Advanced Engineering Technology and Sciences, 09(01), 364–371.

[32] Williamson G and Hall W (1953). X-ray line broadening from filed aluminium and wolfram. Acta Met, 1, 22–31.

[33] Rud A and Lakhnik A (2012). Effect of carbon allotropes on the structure and hydrogen sorption during reactive ball-milling of Mg-C powder mixtures. International Journal of Hydrogen Energy, 37, 4179–4187.

[34] Suryanarayana C (2001). Mechanical alloying and milling. Prog. Mater. Sci, 46, 1–184.

[35] Hussain Z (2021). Comparative study on improving the ball mill process parameters influencing on the synthesis of ultrafine silica sand: a Taguchi coupled optimization technique. International Journal of Precision Engineering and Manufacturing. 22. 10.1007/s12541-021-00492-3.

[36] Rizlan Z and Mamat O (2014). Process parameters optimization of silica sand nanoparticles production using low speed ball milling method. Chinese Journal of Engineering, http://dx.doi.org/10.1155/2014/802459

[37] Zhang F, Zhu M, and Wang C (1994). Atomically disordered nanocrystalline Co_2Si by high-energy ball milling. Journal of Physics Condensed Matter, 6(22), 4043–4052.

[38] Lemine O, Louly M, and Al-Ahmari A (2010). Planetary milling parameters optimization for the production of ZnO nanocrystalline. International Journal of Physical Sciences, 5(17), 2721–2729.

[39] Hajalilou A, Hashim M, Ebrahimi-Kahrizsangi R, Mohamed Kamari H, and Kanagesan S (2014). Parametric optimization of $N\ iF\ e_2O_4$ nanoparticles synthesized by mechanical alloying. Materials Science-Poland, 32, 281–291.

[40] Bilgili E, Hamey R, and Scarlett B (2004). Production of pigment nanoparticles using a wet stirred mill with polymeric media. China Particuology, 93–100.

[41] Taguchi G and Konishi S (1987). Orthogonal arrays and linear graphs. Dearborn: American Supplier Institute.

[42] Phadke M (1989). Quality engineering using robust design. New Jersey: Englewood Cliffs.

[43] Taguchi G, Chowdhury S, and Wu Y (2005). Taguchi's Quality Engineering Handbook. s.l. John Wiley & Sons.

[44] Külekcı M (2013). Analysis of process parameters for a surface-grinding process based on the Taguchi method. Mater. Tehnol, 47, 105–109.

[45] Gill A, Thakur A, and Kumar S (2013). Effect of deep cryogenic treatment on the surface roughness of OHNS die steel after WEDM. International Journal of Applied Engineering Research,7, 1508–1512.

[46] Roy R (2001). Design of experiments using the Taguchi approach. A Wiley-Interscience Publication.

[47] Kowalczyk (2014). Application of Taguchi and ANOVA methods in selection of process parameters for surface roughness in precision turning of titanium. Adv. Manuf. Sci., 38(2).

[48] Roy R (1995). A primer on the Taguchi method. NewYork, Van Nostrand Reinhold.